Aerosol Science and Technology

ISSN: 0278-6826 (Print) 1521-7388 (Online) Journal homepage: https://www.tandfonline.com/loi/uast20

Inactivation of airborne viruses using vacuum ultraviolet photocatalysis for a flow-through indoor air purifier with short irradiation time

Jeonghyun Kim & Jaesung Jang

To cite this article: Jeonghyun Kim & Jaesung Jang (2018) Inactivation of airborne viruses using vacuum ultraviolet photocatalysis for a flow-through indoor air purifier with short irradiation time, Aerosol Science and Technology, 52:5, 557-566, DOI: 10.1080/02786826.2018.1431386

To link to this article: https://doi.org/10.1080/02786826.2018.1431386

AEROSOL SCIENCE AND TECHNOLOGY
2018, VOL. 52, NO. 5, 557–566
https://doi.org/10.1080/02786826.2018.1431386

Inactivation of airborne viruses using vacuum ultraviolet photocatalysis for a flow-through indoor air purifier with short irradiation time

Jeonghyun Kim[a] and Jaesung Jang[a,b]

[a]School of Mechanical, Aerospace and Nuclear Engineering, Ulsan National Institute of Science and Technology, Ulsan, Republic of Korea; [b]Department of Biomedical Engineering, Ulsan National Institute of Science and Technology, Ulsan, Republic of Korea

ABSTRACT

Many ultraviolet (UV)-based disinfection methods have been developed; however, these methods usually use the recirculating mode or need long irradiation periods due to its low photon energy. Vacuum UV (VUV) was recently found to be a promising light source, despite its ozone generation. In this study, we investigated photocatalysis reactions by VUV with short irradiation times (0.004–0.125 s) for simultaneously inactivating airborne MS2 viruses and degrading the generated ozone toward a flow-through air disinfection system with high flow-rates. We developed three effective shapes for the catalyst frame: 2 mm and 5 mm pleated, and spiral-type Pd-TiO_2 catalysts. The 2 mm pleated Pd-TiO_2/VUV photocatalyst exhibited the highest activity for simultaneous MS2 inactivation and ozone degradation, and the catalytic activity was effective regardless of relative humidity. Considering the gas phase and catalyst surface effects, and the natural inactivation of VUV-irradiated but live MS2 viruses, the 2 mm pleated Pd-TiO_2/VUV and succeeding UV photocatalysis showed more than 90% in the overall inactivation efficiency with residual ozone of 35 ppb at an irradiation time of 0.009 s (flow-rate: 33 l/min). In contrast, most UV-based purifiers take longer times for disinfection. This system has the potential for an alternative to conventional UV-based air purifiers.

ARTICLE HISTORY
Received 13 October 2017
Accepted 15 January 2018

EDITOR
Tiina Reponen

1. Introduction

Increasing concerns about pandemics of airborne disease viruses, such as swine influenza virus H1N1 and severe acute respiratory syndrome coronavirus (SARS-CoV), have attracted worldwide attention to cleaning indoor air and spurred the development of air purification techniques for disinfecting airborne viruses and bacteria (Xu et al. 2011). Widely used indoor air purification techniques for disinfection include treatment with non-thermal plasma (NTP), thermal treatment, use of antimicrobial material-embedded filters, ultraviolet (UV) light, and photocatalysis (Xu et al. 2011; Yu et al. 2009). NTP is a partially or fully ionized gas, which can be generated by diverse electrical discharges such as corona discharge, microwave discharge, dielectric barrier discharge, and glow discharge (Lee 2011). In the NTP air-cleaning systems, energetic electrons excite, dissociate, and then ionize gas molecules, generating chemically active species such as atomic oxygen, hydroxyl radicals, and ozone (Yu et al. 2009). These active species inactivate biological particles, eventually forming secondary pollutants (e.g., ozone, CO, or NOx) (Ryan et al. 2010). In thermal treatment, exposure to high temperature denatures proteins by disrupting the structure of polypeptides, resulting in damage to microorganisms (Lee 2011). However, it may consume much power to apply thermal energy at high temperature (Hwang et al. 2010). Filtration systems, in which airborne biological particles are collected on the surface of a filter, are good alternatives to overcome the limitations of the aforementioned techniques. However, these antimicrobial material-embedded filters are generally effective in the short-term because of the accumulation of non-biological dust, they require a large pressure drop, and they must be replaced regularly to prevent the possible re-introduction of airborne microorganisms into the indoor environment (Ryan et al. 2010).

UV photocatalytic oxidation (PCO), an innovative and promising technology, is widely used for air and water disinfection. It has many advantages, including the simultaneous treatment of mixtures of diverse pollutants,

CONTACT Jaesung Jang jjang@unist.ac.kr School of Mechanical, Aerospace and Nuclear Engineering, Ulsan National Institute of Science and Technology (UNIST), Ulsan 44919, Republic of Korea.

Color versions of one or more of the figures in the article can be found online at www.tandfonline.com/uast.
Supplemental files for this article can be found online at the publisher's website.

relatively low cost, and ease of operation and maintenance (Gaya and Abdullah 2008; Pelaez et al. 2012). The most commonly used artificial UV wavelengths in the UV PCO systems are 254 nm and 365 nm, which are considered the UV light sources ideal for disinfection because of their high efficiency for inactivating bacteria and protozoa (Daikoku et al. 2015; Josset et al. 2010; Keller et al. 2005; Lin et al. 2010; Pal et al. 2008; Pigeot-Remy et al. 2014; Rodrigues-Silva et al. 2017). In general, the UV photocatalytic inactivation of bacteria is mainly due to damage of cell walls, membranes, enzymes, and nucleic acids by the reactive oxygen species (ROS) and their stable products (Guo et al. 2012), and virus inactivation under UV PCO is caused by damage to the virus proteins and the genome (Wigginton and Kohn 2012). However, these UV PCO systems still face many challenges, including low photocatalytic activity when the irradiation time is low, electron-hole recombination, and accumulation of refractory intermediates (Fu et al. 2011; Huang and Li 2011).

Recently, vacuum UV (VUV, wavelength $\leq$200 nm) photocatalysis has attracted much attention for air and wastewater treatment applications due to its higher photon energy (6.70 eV) than other UV sources (4.88 and 3.40 eV) having longer UV wavelength (254 and 365 nm) (Fu et al. 2012). VUV light readily breaks down most chemical bonds and generates strong oxidants such as ROS, hydroxyl radicals, and ozone (Huang et al. 2011; Jeong et al. 2004). Nevertheless, the use of VUV light is limited by the generation of toxic ozone (Fu et al. 2011). As ozone is known to cause adverse health effects, the residual ozone generated during VUV photocatalysis must be eliminated (Huang et al. 2011; Oyama and Dhandapani 1997). Among the different techniques to degrade ozone, catalytic decomposition might be a most appropriate one (Park et al. 2011). Previously, noble metals (Pt, Pd, Au) deposited TiO_2 catalysts under VUV irradiation were investigated, in which the effective photocatalytic activity for both volatile organic compounds (VOCs) decomposition and ozone conversion was reported (Fu et al. 2012). In particular, palladium (Pd), usually in the form of nanoparticles, has been found to be a potential photocatalyst for eliminating VOCs. Pd nanoparticles on a TiO_2 catalyst improved the photocatalytic activity by trapping electrons to inhibit the recombination of electron holes, generating strong oxidants such as hydroxyl radicals and reactive oxygen species (Kim et al. 2014).

The majority of studies on UV PCO have focused on water disinfection using TiO_2 aqueous suspensions or self-decontaminating TiO_2 surfaces (Guo et al. 2012; Rincón and Pulgarin 2004; Sunada et al. 1998); only a few studies have been conducted on UV photocatalytic disinfection of airborne bacteria or viruses, which are often called bioaerosols (Daikoku et al. 2015; Josset et al. 2010; Keller et al. 2005; Lin et al. 2010; Pal et al. 2008; Pigeot-Remy et al. 2014; Rodrigues-Silva et al. 2017). Furthermore, VUV photocatalytic inactivation of bioaerosols has not been explored yet (Table 1). In this study, we present a VUV PCO system for simultaneously inactivating airborne viruses and degrading residual ozone, aiming to develop a flow-through air disinfection system with a high flow-rate, which is suitable due to its high photon energy. In this regard, a very short irradiation time ($\leq$0.125 s) was used in this study unlike most previous UV PCO studies. MS2 bacteriophage was selected as the model for this study. It has been widely used as a surrogate airborne virus, as its morphology is similar to that of many pathogenic viruses, including rhinovirus, poliovirus, and foot and mouth disease virus (Hong et al. 2016).

Table 1. Summary of studies on UV photocatalytic oxidation systems for disinfecting bioaerosols.

Light source	Target bioaerosols	Photoreactors	Irradiation time (flow rate)	Disinfection efficiency	Reference
UVA[a]	*Escherichia coli*	TiO_2-coated Pyrex tubular reactor	9–35 s (1.5–6l/min)	99.1–99.8%	(Keller et al. 2005)
UVA[a]	*Escherichia coli*	Continuous annual reactor with TiO_2-coated glass fiber filter	1.1 min (1l/min)	100%	(Pal et al. 2008)
UVA[a]	*Legionella pneumophila*	Three-dimensional solid foam structured reactor	1.5 s (21.6l/min)	94%	(Josset et al. 2010)
UVA[a]	Influenza virus H1N1	TiO_2-coated porous ceramic substrate	5 min (6–24l/min)	100%	(Daikoku et al. 2015)
UVA[a]	*Pseudomonas aeruginosa, Staphylococcus aureus,* Methicillin-resistant *Staphylococcus aureus, Aspergillus fumigatus*	Honeycomb structure made of P25 dip-coated cellulose acetate monoliths	15 min	74–98%	(Rodrigues-Silva et al. 2017)
UVA[a], UVC[b]	*Escherichia coli*	TiO_2-coated glass fiber substrates	~0.5 s (20l/min)	95%	(Lin et al. 2010)
UVA[a], UVC[b]	*Escherichia coli*	TiO_2-coated filter	2–6 h	100%	(Pigeot-Remy et al. 2014)
VUV[c]	MS2 phage	Spiral and pleated Pd-deposited TiO_2 flow-through reactor	0.004–0.125 s (33l/min)	47.8–100%	Present study

[a]UVA: 365 nm wavelength ultraviolet light.
[b]UVC: 254 nm wavelength ultraviolet light.
[c]VUV: 185 nm wavelength ultraviolet light.

The performance of UV photocatalysis is influenced by several factors such as relative humidity (RH), irradiation time, distance between the catalyst and the lamp, shape of the catalyst, specific energy input, ratio of catalyst area to reactor volume (S/V; m^2/m^3), and ratio of reactor volume to the power of the lamp (V/P; m^3/W) (Josset et al. 2010; Mo et al. 2005). In this study, we evaluated the feasibility of a high flow-rate VUV photocatalysis system for inactivating airborne viruses in terms of these factors. In particular, the shape of the catalyst was investigated, as it dictates the effective gas-solid interaction of a VUV-based air purifier. We developed Pd-deposited TiO_2 catalyst frames with different shapes (spiral type and 2 mm and 5 mm pleated type) to improve the contact between the catalyst and the virus-laden air. In addition, UV (at 254 nm wavelength, hereafter referred to simply as UV) photolysis, ozone-combined UV photolysis, and direct ozone treatment were performed to investigate the roles of ozone and UV light of 185 nm wavelength on the inactivation of MS2 bacteriophages in the VUV photocatalysis system. The effects of RH on the inactivation of MS2 bacteriophages and ozone degradation, as well as the change in infectivity of VUV-irradiated but still live MS2 bacteriophages over time at different temperature, were also investigated.

2. Material and methods

2.1. Experimental setup

Figure 1 shows the experimental setup used in this study. The photo-reactor comprised a hollow cylinder made of stainless steel with an inner diameter of 28 mm and a height of 210 mm. A sheet of either TiO_2 or Pd-deposited TiO_2, with a surface area of 150 mm × 90 mm, was fixed to the inner wall of the cylinder. A low-pressure VUV mercury lamp (0.5 W, 1 W, 3 W, 6 W, and 11 W; SANYO UV, Incheon, Korea) with a major emission at 254 nm and a minor emission (ca. 5% of that at 254 nm) at 185 nm was placed along the center of the reactor.

A three-jet Collison nebulizer (Mesa Laboratories, Denver, CO, USA) was used to generate airborne MS2 bacteriophages from a virus stock in deionized water with clean air. The clean air was provided by drying and filtering compressed house air using a clean air supply (Dekati, Finland). The flow rate of the air was controlled using mass flow controllers (MFC, 5850E, Brooks, Hatfield, PA, USA) with an MFC readout box (GMC 1200, ATOVAC, Yongin, Gyeonggi-do, Korea). RH was controlled by passing the air through a thermostatic saturator (RW-0525G, JEIO TECH, Daejeon, Korea). The air flow-rate through the photo-reactor was 33l/min (liter per minute), and the irradiation times calculated from the lamp length and the flow rate at the reaction site were 0.004–0.125 s. A digital micro-manometer (922, Fluke, Everett, WA, USA) was used to measure the pressure drop along the photo-reactor. Airborne MS2 viruses were collected at the inlet and outlet of the photo-reactor using a liquid impinger (Bio-Sampler, SKC Inc., Eighty Four, PA, USA), and the concentrations of viable MS2 viruses were measured by plaque assays, which will be more explained in 2.4. The VUV lamp was switched on after the concentrations at the inlet and outlet became equal and steady, which took approximately 3 h. The ozone was supplied from a VUV photolysis (without catalyst) generator, added to the photo-reactor with MS2 viruses for 0.125 s, and monitored online with an ozone analyzer (Model 49i, Thermo Electron, Franklin, MA, USA).

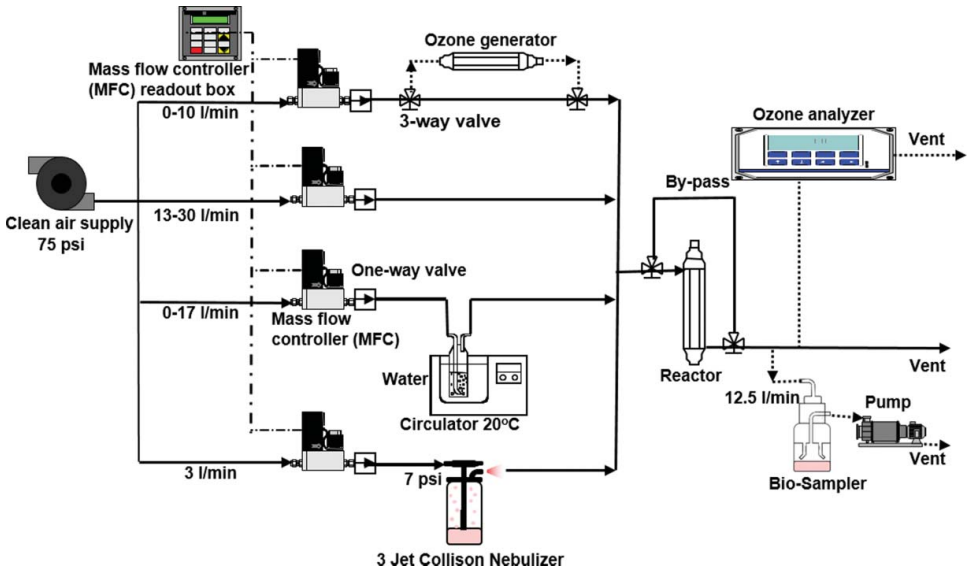

Figure 1. Schematic diagram of the experimental setup.

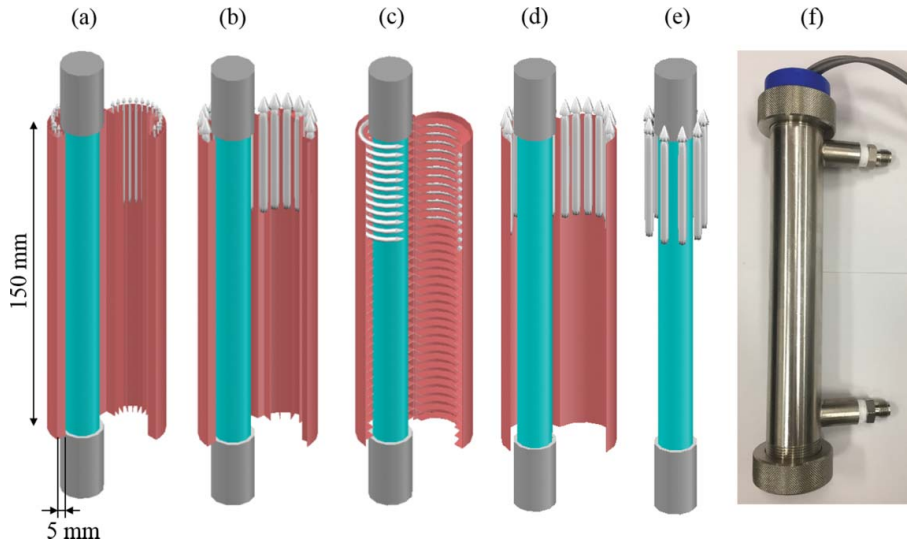

Figure 2. Four types of catalyst frames with an illustration of the gas flow patterns: (a) 2 mm pleated catalyst, (b) 5 mm pleated catalyst, (c) spiral type catalyst, and (d) flat sheet type catalyst. (e) No catalyst. (f) A photograph of the photo-reactor.

2.2. Preparation of catalysts

Four types of catalyst frame shapes (2 mm and 5 mm pleated, spiral, and flat sheet type) were made using 0.2-mm thick titanium (Ti) sheets (Boyuxin, China) (Figure 2). For the pleated type catalysts, many Ti strips (150 mm × 5 mm) were laser-welded in the direction of the air-flow on the inner wall of a cylinder made of a 0.2-mm thick Ti sheet (150 mm × 90 mm) at regularly spaced intervals (2 mm and 5 mm). For the spiral type catalyst, a Ti strip (2,185 mm × 5 mm) was laser-welded in a spiral direction on a 0.2-mm thick Ti sheet (150 mm × 90 mm) at regularly spaced intervals of 5 mm. The distance between the inner surfaces of the catalysts and the VUV lamps was 5 mm. These Ti frames were used as substrates for immobilizing the Pd-TiO_2 catalysts. TiO_2 films were made on the Ti substrates using the sol-gel method, and Pd was deposited on these TiO_2 films using a low-temperature electrostatic self-assembly method described in a previous study (Kim et al. 2014). Briefly, the frames with TiO_2 film were immersed in a Pd colloid solution kept in water at 0°C for 10 min. The colloid solution was prepared by mixing an aqueous solution of polyvinyl alcohol (PVA; 0.02 mm, Junsei) containing $PdCl_2$ (0.6 mm, Sigma Aldrich) with a $NaBH_4$ solution (3.2 mm, Junsei). After immersion, the frames with Pd-TiO_2 film were removed and rinsed with boiling water thrice to remove chloride ions. After completely drying, these frames were heated in air at 300°C for 1 h to remove the capped PVA.

2.3. Preparation and enumeration of MS2 bacteriophages

All media, reagents, and glassware used for the culture preparation were initially sterilized by autoclaving at 121°C for 15 min. The MS2 bacteriophage (15597-B1, ATCC) was used as a surrogate for airborne viruses in this study (Hong et al. 2016). *Escherichia coli* C3000 (15597, ATCC) was chosen as the host bacterium. First, to cultivate the MS2 bacteriophage, the host bacteria were inoculated in 20 ml of tryptic soy broth (TSB, 211825, Becton, Dickinson and Company) and incubated while shaking at 160 rpm and 37°C for 12 h. For the propagation of phages, freeze-dried MS2 phages were dissolved in 1 × phosphate-buffered saline (PBS, pH 7.4, GIBCO) at a concentration of 1 mg/ml. The resultant MS2 suspension (500 μl) was added to 10 ml of the *E. coli* C3000 culture, and this mixture was further incubated at 160 rpm and 37°C for 6 h. After propagation, the mixture was centrifuged at 3000 rpm (Centrifuge FLETA 5, Hanil, Korea) for 10 min to separate the bacterial cells and their debris from the MS2 suspension. The supernatant was filtered thrice through membrane filters with 0.22-μm pores (4612, Pall Corporation). The filtered MS2 stock suspension at a concentration of 10^{11} plaque-forming units (PFU)/ml was stored at −20°C, until further use. Finally, the suspension for nebulization was made by adding 100 μl of the stock to 99.9 ml of deionized water. The concentration of viable MS2 phages in the suspension was measured to be 2.30 (±. 27) × 10^8 PFU/ml.

2.4. Bioaerosol sampling, quantification, and analysis

Each air sample was collected at the reactor outlet using a liquid impinger (BioSampler, SKC Inc., Eighty Four) with 20 ml of 1 × PBS solution for 10 min. A vacuum pump (Tanker215, Roker) was used at a flow rate of

12.5l/min for this impinger. Before sampling, the air flow of the impinger was calibrated with a bubble flowmeter (2048-U, SUPELCO Analytical). After sampling, the acquired sample suspensions were stored at 4°C until further analysis.

For quantifying the concentration of MS2 in the samples, early log-phase cultures in a TSB medium with 1.5% broth agar were used, based on the plaque assay method according to the ISO 10705-1 guidelines. Briefly, 20 ml of the broth agar was poured onto a 90-mm diameter petri dish and allowed to solidify. After solidification, 200 μl of the previously prepared *E. coli* C3000 culture suspension was uniformly spread on the broth agar surface. The collected MS2 suspension (100 μl) was pipetted onto the agar plate and allowed to solidify. The agar plate was then incubated upside-down at 37°C for 5 h, and the MS2 plaques were counted. This was also used to determine the concentration of MS2 stock solution.

To assess the effect of the catalyst frame shapes on MS2 inactivation and ozone degradation, the efficiencies were calculated as follows:

$$\text{MS2 inactivation efficiency (\%)} = \frac{[PFU]_{before\ reaction} - [PFU]_{after\ reaction}}{[PFU]_{before\ reaction}} \times 100$$

$$\text{Ozone degradation efficiency (\%)} = \frac{[O_3]_{VUV} - [O_3]_{catalyst}}{[O_3]_{VUV}} \times 100$$

where $[PFU]_{before\ reaction}$ is the concentration of live MS2 before reaction with VUV, UV, or ozone; $[PFU]_{after\ reaction}$ is the concentration of live MS2 after the reaction; $[O_3]_{VUV}$ is the outlet concentration of the ozone generated by the VUV lamp in the absence of catalysts; and $[O_3]_{catalyst}$ is the concentration of ozone in the presence of a catalyst.

2.5. Experimental procedure

Generally, UV photocatalysis reactions occur heterogeneously both in the gas phase and on the catalyst surface (Kim et al. 2014). Firstly, only the gas phase reaction was explored to study the role of VUV light in VUV photocatalysis. The gas phase reaction under VUV light involves light of 185 nm wavelength, light of 254 nm wavelength, ozone oxidation, water ionization, and subsequent attack of reactive oxidant species (Huang et al. 2016) since commercial VUV lamps generally emit both 185 nm and 254 nm wavelength components, with photon energies of 6.70 eV and 4.88 eV, respectively (Zhang et al. 2004). Light of 185 nm wavelength and residual ozone are both typical of the VUV photolysis process. In order to identify the component responsible for the inactivation, MS2 inactivation efficiency at short irradiation times were compared in four treatments: $VUV_{185+254\ nm}$ light (VUV photolysis without photocatalyst), $UV_{254\ nm}$ light (UV photolysis), ozone dose combined with UV photolysis (ozone + $UV_{254\ nm}$ light), and ozone dose treatment alone.

Three more tests were then conducted to investigate the effects of the catalyst shape on the MS2 inactivation and ozone degradation. The first test aimed to compare the photocatalytic activities of conventional plate type catalysts with two different materials: TiO_2 catalyst and Pd nanoparticle-deposited TiO_2 (hereafter referred to as Pd-TiO_2) catalyst. Thus, we evaluated the effects of Pd nanoparticles on TiO_2 catalyst. Second, the photocatalytic efficiencies of four catalyst frame shapes (2 mm pleated Pd-TiO_2 catalyst, 5 mm pleated Pd-TiO_2 catalyst, and spiral type Pd-TiO_2 catalyst) were evaluated in order to improve the plate type Pd-TiO_2 catalyst. Finally, for practical application of VUV photocatalysis, we evaluated the combined effect of VUV photocatalysis followed by UV photocatalysis.

2.6. Statistical analysis

All experiments were conducted in triplicate. The average values of the data are shown in the figures, and their standard deviations are indicated as error bars. The normality of the data distribution was checked using Kolmogorov-Smirnov test, and all data were normally distributed. Statistical analyses were performed using one-way analysis of variance (ANOVA) followed by Tukey's post hoc test. Results with $p < 0.05$ were considered statistically significant.

3. Results and discussion

3.1. Comparison between $VUV_{185+254\ nm}$ light, $UV_{254\ nm}$ light, ozone dose + $UV_{254\ nm}$ light combination, and ozone dose

Figure 3a shows the MS2 inactivation efficiency with irradiation time for all four treatments. The highest MS2 inactivation efficiency was obtained with VUV photolysis for all the tested irradiation times. Even when the irradiation time was decreased to 0.009 s and 0.004 s, VUV photolysis (185 nm and 254 nm wavelength components) showed significant MS2 inactivation efficiency, which may be due to the high photon energy of 185 nm VUV light, compared to the UV photolysis (254 nm wavelength component). In fact, the inactivation

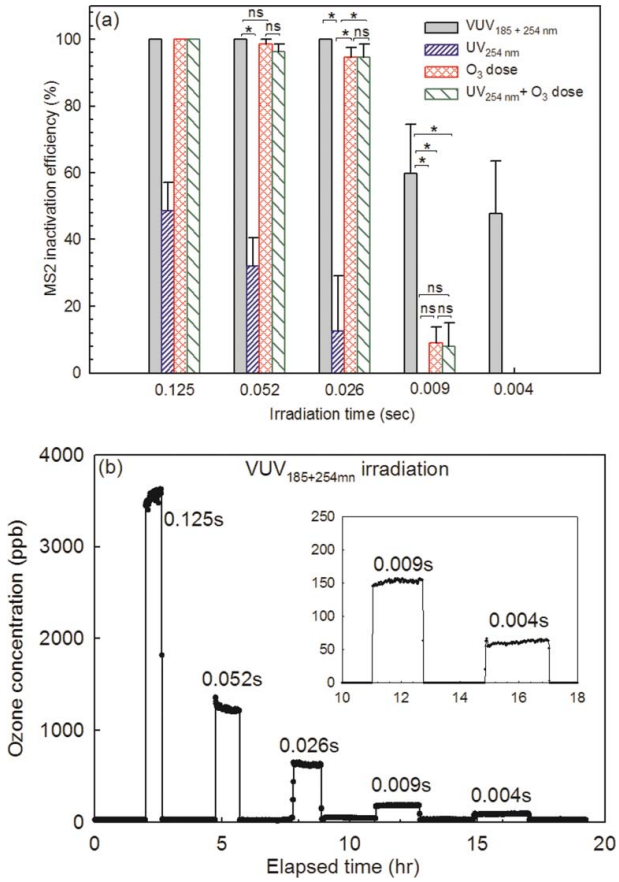

Figure 3. (a) Dependence of MS2 inactivation efficiency on irradiation time for four treatments. (b) Concentration of ozone generated with different VUV irradiation times. Experimental conditions: flow rate = 33l/min, $[MS2]_{inlet} = 1.7 \times 10^3$ PFU/ml, RH = 40%, n = 3, $^{*}P < 0.05$, ns: $P \geq 0.05$.

efficiency of the UV photolysis was approximately 10% of that of the VUV photolysis at an irradiation time of 0.026 s. Due to its high photon energy, 185 nm VUV light directly breaks down most chemical bonds, and dissociates oxygen and water molecules in the gas phase, thus generating more reactive oxidants (such as ·OH, O·, and O_3) than UV light (Fu et al. 2012; Kim et al. 2014). The reactive oxidants can lead to the virus inactivation through the sufficient damage to either the protein or nucleic acid structure (Equations 1–10 in the online supplemental information).

Ozone, which is also known to inactivate viruses, is generated during VUV irradiation ([E3]-[E5]), and reactive oxidants are generated from ozone dissociation under $UV_{254\ nm}$ ([E7], [E8]). To analyze the contribution of the ozone generated in the VUV photolysis to the MS2 inactivation, we compared with the ozone dose combined with UV photolysis and the ozone dose treatment only for different ozone dose concentrations (60 – 3,537 ppb) (Figure 3a). These two treatments exhibited almost the same inactivation efficiencies, and hence UV photolysis did not contribute to the inactivation compared to the ozone dose treatment. In the ozone dose treatment, the used ozone concentration at each irradiation time (Figure 3a) was the same as the ozone concentration generated from VUV photolysis with the same irradiation time (Figure 3b). When the ozone concentration was decreased to 150 ppb, which was generated when VUV light was irradiated for 0.009 s, the MS2 inactivation efficiency sharply decreased, and ozone dose treatment showed approximately 6 times lower MS2 inactivation efficiency than VUV photolysis. These results indicated that the effect of reactive oxidants generated from ozone dissociation ([E7], [E8]) was not stronger than that of the 185 nm wavelength component in the gas phase; furthermore, the reaction of the ozone dose combined with UV photolysis was governed by ozone oxidation ([E3]-[E6]). The MS2 inactivation efficiency significantly increased as the inlet ozone concentration increased. When the ozone concentration was higher than approximately 1,227 ppb (at an irradiation time of 0.052 s), most MS2 bacteriophages were completely inactivated. However, due to high toxicity, this concentration of ozone is not permitted in the indoor environment. Based on these results, we concluded that MS2 inactivation under VUV light was

governed by the 185 nm wavelength component, and that VUV light could be an effective light source for purifying indoor air, even with very short irradiation times.

In addition, when the specific energy input (i.e., the energy required to disinfect airborne viruses) was increased from 0.25 Wh/m^3 to 5.56 Wh/m^3, the MS2 inactivation efficiency increased from 48% to 100% for VUV photolysis and from 0% to 48% for UV photolysis (Table 2). Despite the same MS2 inactivation efficiencies, the specific energy input for the VUV photolysis was lower than that for the UV photolysis, and the irradiation time of VUV photolysis was shortened by 31 times. Because of this low virus inactivation efficiency at short irradiation time, most studies on conventional (254 nm or 365 nm wavelength) UV-based air purifiers are conducted in the recirculating mode with relatively long irradiation times (Grinshpun et al. 2007; Xu et al. 2005). However, the flow rates in typical air-purifiers are several meters-cubed per minute, corresponding to an irradiation time of less than approximately 0.1 s (Shaughnessy and Sextro 2006; Zhang et al. 2011). Therefore, VUV photolysis would be very attractive for practical applications in UV-based HVAC (heating, ventilation, air conditioning) purifiers.

3.2. Effects of catalyst surface and frame shape

Firstly, we compared the photocatalytic activities of TiO_2 catalyst with those of Pd-TiO_2 catalyst under VUV irradiation; they were also compared with VUV photolysis (without catalyst) (Figure 4). No significant differences in MS2 inactivation were observed between these three groups; however, ozone degradation was increased by 14% and 21% when plate TiO_2 and Pd-TiO_2 catalysts were used, respectively. These results indicated that, although Pd deposition did not improve MS2 inactivation, it greatly improved ozone degradation, even at short irradiation times. Based on these results, we speculated that photochemical reactions on the surface of Pd-TiO_2 catalysts occur in two pathways: TiO_2 surface and deposited Pd nanoparticles (Equations 11–19 in the supplemental information).

Table 2. Specific energy input versus MS2 inactivation.

Irradiation time (s)	Specific energy input (Wh/m^3)	MS2 inactivation efficiency (%)	
		VUV	UV
0.125	5.56	100	48
0.052	3.08	100	32
0.026	1.52	100	12
0.009	0.51	60	0
0.004	0.25	48	0

Experimental conditions: flow rate = 33l/min, $[MS2]_{inlet} = 1.7 \times 10^3$ PFU/ml, RH = 40%.

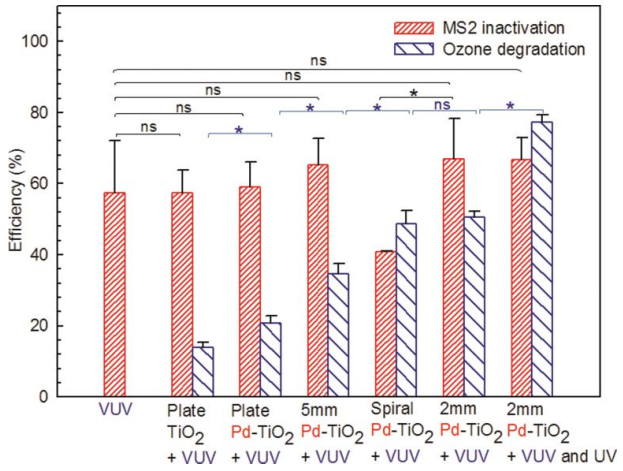

Figure 4. Dependence of MS2 inactivation and ozone degradation on catalyst frame shape. Experimental conditions: $[MS2]_{inlet} = 1.7 \times 10^3$ PFU/ml, $[O_3]_{VUV} = 152$ ppb, RH = 40%, flow rate = 33l/min, n = 3, $^*P < 0.05$, ns: $P \geq 0.05$.

Although the plate-type Pd-TiO_2 with VUV photocatalysis showed higher photocatalytic activity than the plate-type TiO_2 with VUV photocatalysis, it generated 110 ppb of residual ozone (with 20.7% ozone degradation efficiency). According to the California Air Resources Board (CARB 2009), the permissible ozone emission limit for indoor air cleaning devices is 50 ppb. Therefore, to improve the ozone degradation of the Pd-TiO_2 catalyst further, we designed three kinds of catalyst frame shapes (2 mm pleated Pd-TiO_2 catalyst, 5 mm pleated Pd-TiO_2 catalyst, and spiral type Pd-TiO_2 catalyst), and evaluated their photocatalytic activities for MS2 inactivation and ozone degradation with fixed volume flow rates (Figure 4 and Table 3).

The photocatalytic activity of Pd-TiO_2 for the simultaneous inactivation of MS2 and degradation of residual ozone was found to be dependent on the ratio of S/V, and the space velocity. A higher catalyst surface area and higher ratio of S/V resulted in higher ozone degradation; when the ratio of S/V increased from 2.0×10^5 to 8.3×10^5, the ozone degradation efficiency increased from 20.7% to 50.5%. In addition, although the spiral type Pd-TiO_2 catalyst had a high S/V ratio, it exhibited the lowest MS2 inactivation efficiency and high space velocity. This may be due to insufficient reaction time for MS2 inactivation in the gas phase. These results indicated that MS2 bacteriophages were inactivated by VUV light in the gas phase, and that the ozone was degraded by the catalyst surface. Thus, high S/V ratio and low space velocity improved the ozone degradation and MS2 inactivation of the VUV photocatalysis reactor, respectively.

Ozone can also be degraded by UV light of 254 nm wavelength ([E7]) with Pd-TiO_2 catalyst immediately after VUV photocatalysis (2 mm pleated Pd-TiO_2/VUV)

Table 3. Specifications of the Pd-TiO_2 photo-reactors used in the present study.

Catalyst frame shape	Catalyst surface area[a] (m^2)	S/V[b] (m^2/m^3)	Ozone degradation efficiency (%)	MS2 inactivation efficiency (%)	Space velocity[c] (/s)	Pressure drop (kPa)
2 mm pleated catalyst	0.0506	8.3×10^5	50.5 ± 1.8	66.9 ± 11.4	161.8	3.6 ± 0.007
5 mm pleated catalyst	0.0314	5.1×10^5	34.7 ± 2.8	65.4 ± 7.4	133.7	3.6 ± 0.001
Spiral type catalyst	0.0399	6.2×10^5	48.8 ± 3.7	40.9 ± 0.1	193.9	3.8 ± 0.034
Plate sheet catalyst	0.0134	2.0×10^5	20.7 ± 2.2	59.1 ± 7.0	120.8	3.6 ± 0.007
No catalyst	—	—		57.3 ± 14.8	—	3.6 ± 0.007

[a]Sectional area of the reactor.
[b]Ratio of catalyst area to reactor volume.
[c]Space velocity is defined as the volumetric flow rate of the feed gas divided by the catalyst volume. Experimental conditions: flow rate = 33l/min, RH = 40%, $[MS2]_{inlet} = 1.7 \times 10^3$ PFU/ml, $[O_3]_{VUV} = 152$ ppb, n = 3.

(Figure 4). The following UV light of 254 nm wavelength under Pd-TiO_2 catalyst did not enhance the photocatalytic activity of MS2 inactivation, compared to the inactivation efficiency of the 2 mm pleated Pd-TiO_2/VUV photocatalyst, implying that the UV light in the system did not inactivate the MS2 at a flow rate of 33l/min. In contrast, the extra UV photocatalysis exhibited a remarkable ozone degradation efficiency (77.3%, with an ozone concentration of 35 ppb), which is less than the CARB ozone emission limit. These results indicated that the VUV+UV combination photocatalysis caused a series of chain reactions, including ozone generation and its subsequent degradation ([E3]-[E10]). Therefore, this VUV + UV combination system can be used for indoor air purification systems with high flow rates and short irradiation times.

3.3. Effects of RH

RH is considered an important variable for UV-based purification of indoor air (Arundel et al. 1986; Peccia et al. 2001). High RH has been reported to be beneficial, as it generates high amounts of hydroxyl radicals, thus improving UV inactivation (Pal et al. 2008). However, other studies have shown a significant decrease in UV inactivation rates at high RH levels due to competitive adsorption of H_2O and organic molecules (Peccia et al. 2001). In this study, to simulate dry and rainy conditions, 2 mm pleated Pd-TiO_2/VUV photocatalysis was performed at RH levels of 10%, 40%, and 70% (Figure 5). Apart from a slight decrease in MS2 inactivation at 70% RH, MS2 inactivation and ozone degradation in the 2 mm pleated Pd-TiO_2/VUV photocatalysis showed no significant differences in these RH levels. These RH effects on the MS2 inactivation may be attributed to the hydrophobicity of Pd-TiO_2. In fact, Pd nanoparticles on the surface of TiO_2 catalyst exhibited hydrophobic property (Fu et al. 2011), which can inhibit the adsorption of MS2 viruses and water molecules degrading the Pd-TiO_2/VUV photocatalysis. These results suggest that the VUV photocatalysis system with 2 mm pleated Pd-TiO_2 catalyst can be used for practical HVAC systems, regardless of RH.

3.4. Indirect effects of VUV light

The change in viability of VUV-irradiated but still live viruses with time is important, especially if they are pathogenic. The last experiment in this study was conducted to evaluate the effects of time and temperature on the natural inactivation of MS2 bacteriophages that were subject to VUV-irradiation with the 2 mm pleated Pd-TiO_2 photocatalyst. To evaluate these effects indirectly, we passed the bacteriophages through the photo-reactor with and without VUV photocatalysis, collected them with a BioSampler, stored them for 1–12 h at 4 and 25°C, and quantified the PFUs formed (Figure 6). When the viruses were collected without VUV irradiation, the MS2 inactivation rate, or the ratio C_t/C_o, at 25°C was higher than that at 4°C; however, the natural inactivation rates eventually reached similar levels, 53% and 55%, at 4°C and 25°C, respectively, after 12 h. In contrast, the concentration of viable MS2 viruses VUV-irradiated decreased to approximately 30% of the initial concentration, irrespective of storage temperature, and was lower than that of non-irradiated ones. Considering the effects of the gas phase and catalyst surface (66.9% in the MS2

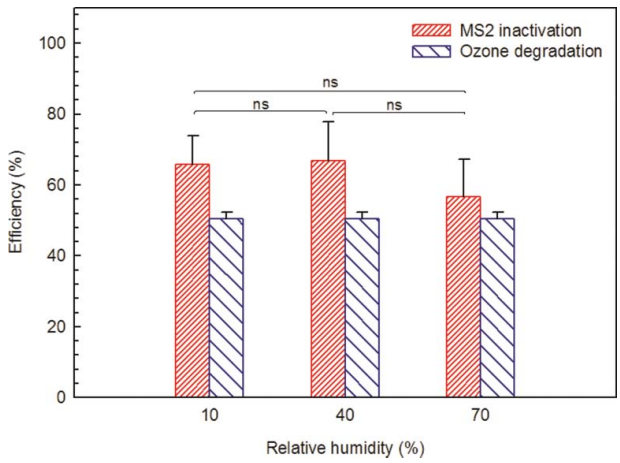

Figure 5. The effect of RH on MS2 inactivation and O_3 degradation. Experimental conditions: $[MS2]_{inlet} = 1.7 \times 10^3$ PFU/ml, $[O_3]_{VUV\ with\ catalyst} = 65$ ppb, irradiation time = 0.009 s, flow rate = 33l/min, n = 3, *: $P < 0.05$, ns: $P \geq 0.05$.

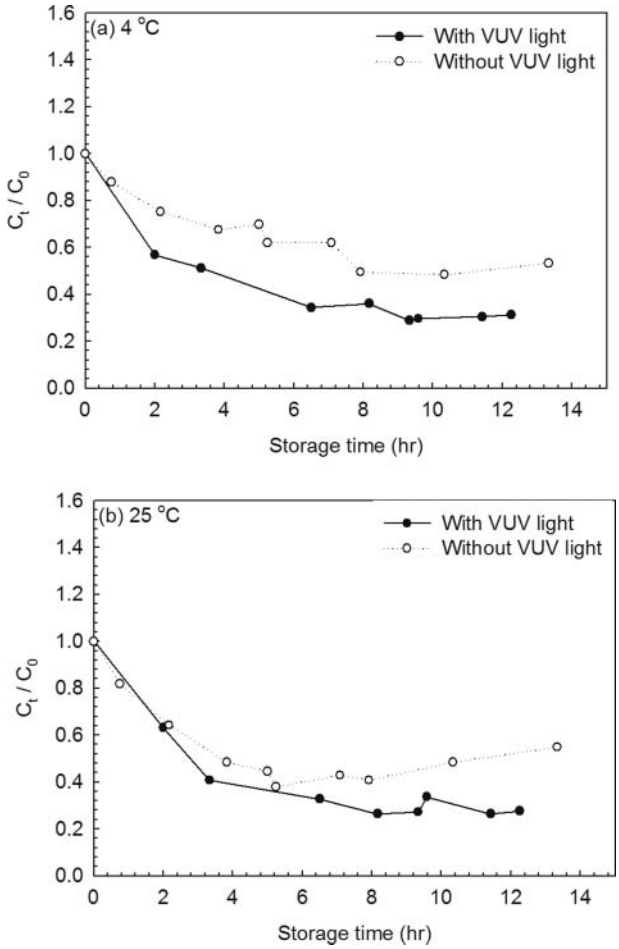

Figure 6. Natural decay of MS2 infectivity, with and without VUV irradiation, as a function of storage time at (a) 4°C and (b) 25°C, where C_o and C_t are the concentrations of viable MS2 viruses at collection and storage time t, respectively. Experimental conditions: flow rate = 33l/min, $[MS2]_{No\ Treatment} = 1.7 \times 10^3$ PFU/ml, $[MS2]_{VUV\ with\ catalyst} = 4.1 \times 10^2$ PFU, RH = 40%, irradiation time = 0.009s, n = 3.

inactivation efficiency), and the indirect effects of VUV light (ca. 70% in the MS2 inactivation efficiency), VUV inactivation efficiency for MS2 bacteriophages reached more than 90% with an irradiation time of 0.009s. Thus, VUV photocatalysis using 2 mm pleated Pd-TiO_2 catalyst can be an effective platform for simultaneous MS2 inactivation and ozone degradation, with very short irradiation times.

4. Conclusions

In this study, we explored VUV photocatalysis for simultaneously inactivating airborne MS2 viruses and degrading ozone, using effective catalyst frames (2 mm and 5 mm pleated, and spiral-type Pd-TiO_2 catalysts) and short irradiation times (0.004–0.125s). Compared with UV photolysis, ozone dose combined with UV photolysis, and ozone dose alone treatments, VUV photolysis treatment showed the highest inactivation efficiencies for MS2 viruses. Regarding the tested catalyst frames, the 2 mm pleated Pd-TiO_2 catalyst was the most effective in inactivating MS2 viruses (more than 90% in the overall inactivation efficiency) under VUV irradiation at an irradiation time of 0.009 s (flow-rate: 33 lpm), contrasting with conventional UV irradiation. In addition, the subsequent 2 mm pleated Pd-TiO_2/UV photocatalysis process further degraded the residual ozone, such that the final level (35 ppb) was below the CARB ozone emission limit. This system has the potential for high-capacity bioaerosol inactivation in HVAC systems, regardless of the weather.

Funding

This research was supported by Basic Science Research Program through the National Research Foundation of Korea (NRF) funded by the Ministry of Science, ICT and Future Planning (#2015R1A2A2A01006446), and the 2017 Research Fund (1.170013.01) of UNIST.

References

Arundel, A. V., Sterling, E. M., Biggin, J. H., and Sterling, T. D. (1986). Indirect health effects of relative humidity in indoor environments. *Environ. Health Perspect.*, 65:351.

CARB. (2009). Regulation for limiting ozone emissions from indoor air cleaning devices, California Air Resources Board.

Daikoku, T., Takemoto, M., Yoshida, Y., Okuda, T., Takahashi, Y., Ota, K., Tokuoka, F., Kawaguchi, A. T., and Shiraki, K. (2015). Decomposition of organic chemicals in the air and inactivation of aerosol-associated influenza infectivity by photocatalysis. *Aerosol Air Qual. Res.*, 15:1469–1484. doi:10.4209/aaqr.2014.10.0256.

Fu, P. F., Zhang, P. Y., and Li, J. (2011). Photocatalytic degradation of low concentration formaldehyde and simultaneous elimination of ozone by-product using palladium modified TiO_2 films under UV254+185 nm irradiation. *Appl. Catal. B.*, 105:220–228. doi:10.1016/j.apcatb.2011.04.021.

Fu, P. F., Zhang, P. Y., and Li, J. (2012). Simultaneous elimination of formaldehyde and ozone byproduct using noble metal modified TiO_2 films in the gaseous VUV photocatalysis. *Int. J. Photoenergy.*, 2012:1–8. doi:10.1155/2012/174862.

Gaya, U. I., and Abdullah, A. H. (2008). Heterogeneous photocatalytic degradation of organic contaminants over titanium dioxide: a review of fundamentals, progress and problems. *J. Photochem. Photobiol. C.*, 9:1–12. doi:10.1016/j.jphotochemrev.2007.12.003.

Grinshpun, S. A., Adhikari, A., Honda, T., Kim, K. Y., Toivola, M., Ramchander Rao, K., and Reponen, T. (2007). Control of aerosol contaminants in indoor air: combining the particle concentration reduction with microbial inactivation. *Environ. Sci. Technol.*, 41:606–612. doi:10.1021/es061373o.

Guo, M.-Z., Ling, T.-C., and Poon, C.-S. (2012). TiO_2-based self-compacting glass mortar: comparison of photocatalytic

nitrogen oxide removal and bacteria inactivation. *Build. Environ.*, 53:1–6. doi:10.1016/j.buildenv.2011.12.022.

Hong, S., Bhardwaj, J., Han, C.-H., and Jang, J. (2016). Gentle sampling of submicrometer airborne virus particles using a personal electrostatic particle concentrator. *Environ. Sci. Technol.*, 50:12365–12372. doi:10.1021/acs.est.6b03464.

Huang, H., and Li, W. (2011). Destruction of toluene by ozone-enhanced photocatalysis: Performance and mechanism. *Appl. Catal. B*, 102:449–453. doi:10.1016/j.apcatb.2010.12.025.

Huang, H., Lu, H., Huang, H., Wang, L., Zhang, J., and Leung, D. Y. C. (2016). Recent development of VUV-based processes for air pollutants degradation. *Front. Environ. Sci.*, 4:1–13.

Huang, H. B., Leung, D. Y. C., Li, G. S., Leung, M. K. H., and Fu, X. L. (2011). Photocatalytic destruction of air pollutants with vacuum ultraviolet (VUV) irradiation. *Catal. Today*, 175:310–315. doi:10.1016/j.cattod.2011.04.015.

Hwang, G. B., Jung, J. H., Jeong, T. G., and Lee, B. U. (2010). Effect of hybrid UV-thermal energy stimuli on inactivation of *S. epidermidis* and *B. subtilis* bacterial bioaerosols. *Sci. Total Environ.*, 408:5903–5909. doi:10.1016/j.scitotenv.2010.08.016.

Jeong, J. Y., Sekiguchi, K., and Sakamoto, K. (2004). Photochemical and photocatalytic degradation of gaseous toluene using short-wavelength UV irradiation with TiO_2 catalyst: comparison of three UV sources. *Chemosphere*, 57:663–671. doi:10.1016/j.chemosphere.2004.05.037.

Josset, S., Hajiesmaili, S., Begin, D., Edouard, D., Pham-Huu, C., Lett, M.-C., Keller, N., and Keller, V. (2010). UV-A photocatalytic treatment of Legionella pneumophila bacteria contaminated airflows through three-dimensional solid foam structured photocatalytic reactors. *J. Hazard. Mater.*, 175:372–381. doi:10.1016/j.jhazmat.2009.10.013.

Keller, V., Keller, N., Ledoux, M. J., and Lett, M.-C. (2005). Biological agent inactivation in a flowing air stream by photocatalysis. *Chem. Commun.*, 23:2918–2920. doi:10.1039/b503638k.

Kim, J., Zhang, P., Li, J., Wang, J., and Fu, P. (2014). Photocatalytic degradation of gaseous toluene and ozone under UV254+185 nm irradiation using a Pd-deposited TiO_2 film. *Chem. Eng. J.*, 252:337–345. doi:10.1016/j.cej.2014.05.015.

Lee, B. U. (2011). Life comes from the air: a short review on bioaerosol control. *Aerosol Air Qual. Res.*, 11:921–927.

Lin, C.-H., Lee, J.-W., Chang, C.-Y., Chang, Y.-J., Lee, Y.-C., and Hwa, M.-Y. (2010). Novel TiO_2 thin films/glass fiber photocatalytic reactors in the removal of bioaerosols. *Surf. Coat. Technol.*, 205:S341–S344. doi:10.1016/j.surfcoat.2010.08.009.

Mo, J., Zhang, Y., and Yang, R. (2005). Novel insight into VOC removal performance of photocatalytic oxidation reactors. *Indoor Air.*, 15:291–300. doi:10.1111/j.1600-0668.2005.00374.x.

Oyama, S. T., and Dhandapani, B. (1997). Gas phase ozone decomposition catalysts. *Appl. Catal. B*, 11:129–166. doi:10.1016/S0926-3373(96)00044-6.

Pal, A., Pehkonen, S. O., Yu, L. E., and Ray, M. B. (2008). Photocatalytic inactivation of airborne bacteria in a continuous-flow reactor. *Ind. Eng. Chem. Res.*, 47:7580–7585. doi:10.1021/ie701739g.

Park, E., Chin, S., Kim, J., Bae, G.-N., and Jurng, J. (2011). Preparation of $MnOx/TiO_2$ ultrafine nanocomposite with large surface area and its enhanced toluene oxidation at low temperature. *Powder Technol.*, 208:740–743. doi:10.1016/j.powtec.2011.01.001.

Peccia, J., Werth, H. M., Miller, S., and Hernandez, M. (2001). Effects of relative humidity on the ultraviolet induced inactivation of airborne bacteria. *Aerosol Sci. Technol.*, 35:728–740. doi:10.1080/02786820152546770.

Pelaez, M., Nolan, N. T., Pillai, S. C., Seery, M. K., Falaras, P., Kontos, A. G., Dunlop, P. S., Hamilton, J. W., Byrne, J. A., and O'shea, K. (2012). A review on the visible light active titanium dioxide photocatalysts for environmental applications. *Appl. Catal. B*, 125:331–349. doi:10.1016/j.apcatb.2012.05.036.

Pigeot-Remy, S., Lazzaroni, J., Simonet, F., Petinga, P., Vallet, C., Petit, P., Vialle, P., and Guillard, C. (2014). Survival of bioaerosols in HVAC system photocatalytic filters. *Appl. Catal. B*, 144:654–664. doi:10.1016/j.apcatb.2013.07.036.

Rincón, A.-G., and Pulgarin, C. (2004). Bactericidal action of illuminated TiO_2 on pure Escherichia coli and natural bacterial consortia: post-irradiation events in the dark and assessment of the effective disinfection time. *Appl. Catal. B*, 49:99–112. doi:10.1016/j.apcatb.2003.11.013.

Rodrigues-Silva, C., Miranda, S. M., Lopes, F. V., Silva, M., Dezotti, M., Silva, A. M., Faria, J. L., Boaventura, R. A., Vilar, V. J., and Pinto, E. (2017). Bacteria and fungi inactivation by photocatalysis under UVA irradiation: liquid and gas phase. *Environ. Sci. Pollut. Res.*, 24:6372–6381. doi:10.1007/s11356-016-7137-8.

Ryan, K., McCabe, K., Clements, N., Hernandez, M., and Miller, S. L. (2010). Inactivation of airborne microorganisms using novel ultraviolet radiation sources in reflective flow-through control devices. *Aerosol Sci. Technol.*, 44:541–550. doi:10.1080/02786821003762411.

Shaughnessy, R., and Sextro, R. (2006). What is an effective portable air cleaning device? A review. *J. Occup. Environ.l Hyg.* 3:169–181. doi:10.1080/15459620600580129.

Sunada, K., Kikuchi, Y., Hashimoto, K., and Fujishima, A. (1998). Bactericidal and detoxification effects of TiO_2 thin film photocatalysts. *Environ. Sci. Technol.*, 32:726–728. doi:10.1021/es970860o.

Wigginton, K. R., and Kohn, T. (2012). Virus disinfection mechanisms: the role of virus composition, structure, and function. *Curr. Opin. Virol.*, 2:84–89. doi:10.1016/j.coviro.2011.11.003.

Xu, P., Kujundzic, E., Peccia, J., Schafer, M. P., Moss, G., Hernandez, M., and Miller, S. L. (2005). Impact of environmental factors on efficacy of upper-room air ultraviolet germicidal irradiation for inactivating airborne mycobacteria. *Environ. Sci. Technol.*, 39:9656–9664. doi:10.1021/es0504892.

Xu, Z., Wu, Y., Shen, F., Chen, Q., Tan, M., and Yao, M. (2011). Bioaerosol science, technology, and engineering: past, present, and future. *Aerosol Sci. Technol.*, 45:1337–1349. doi:10.1080/02786826.2011.593591.

Yu, B., Hu, Z., Liu, M., Yang, H., Kong, Q., and Liu, Y. (2009). Review of research on air-conditioning systems and indoor air quality control for human health. *Int. J. Refrig.*, 32:3–20. doi:10.1016/j.ijrefrig.2008.05.004.

Zhang, P. Y., Liu, J., and Zhang, Z. L. (2004). VUV photocatalytic degradation of toluene in the gas phase. *Chem. Lett.*, 33:1242–1243. doi:10.1246/cl.2004.1242.

Zhang, Y., Mo, J., Li, Y., Sundell, J., Wargocki, P., Zhang, J., Little, J. C., Corsi, R., Deng, Q., Leung, M. H. K., Fang, L., Chen, W., Li, J., and Sun, Y. (2011). Can commonly-used fan-driven air cleaning technologies improve indoor air quality? A literature review. *Atmos. Environ.*, 45:4329–4343. doi:10.1016/j.atmosenv.2011.05.041.